Fast Model-based Design of High Performance Permanent Magnet Machine for Next Generation Electric Propulsion for Urban Aerial Vehicle Application

Sarbajit Paul, *Student Member, IEEE*, and Junghwan Chang, *Member, IEEE*

***Abstract*—Model order reduction (MOR) is considered as a good alternative to reduce the computational scale for electro-magnetic problems. The aim of this work is to introduce the use of dynamic mode decomposition (DMD) as a promising tool for MOR to analyze its effectiveness in creating a fast model-based design platform for the permanent magnet motor design for ur-ban aerial vehicles (UAVs). Using a singular value decomposition (SVD) based DMD, the design process is constructed and verified against different scenarios.**

***Index Terms*—Dynamic mode decomposition, model order reduction, permanent magnet synchronous motor, urban aerial vehicles.**

I. INTRODUCTION

THERE is an increased concern around the world to reduce the use of conventional sources of energy such as the combustion of fossil fuels. This has raised alarming concern for the transportation and aeronautical industries. Furthermore, the use of fossil fuel causes severe long-term environmental effects such as air pollution, global warming and ozone layer depletion etc. [1, 2]. Thus, there is tremendous market push for more greener, more efficient, more sustainable, and alter-native sources, technologies and polices for the transportation industries world-wide. Since last one decade, the automotive industry has successfully transformed outlook for the public and personal transport by using hybrid and pure electric solutions. Based on the European Commission's flight-path 2050, carbon dioxide emissions must be decreased by 75%[3]. Similarly, the aviation industry is also facing the challenge to reduce its carbon footprint as the global estimation shows 2% of total fuel consumption in the transportation sector is by the aviation industry and is expected to increase to 11-12% by 2050.

Manuscript received October 20, 2020; revised March 15, 2021; accepted June 01, 2021. date of publication June 25, 2021; date of current version June 18, 2021.

This work was supported by Dong-A University research fund. *(Corresponding author: J. Chang)*

Sarbajit Paul and Junghwan Chang are with Mechatronics System Research Lab, Electrical Engineering Department, Dong-A University, Busan, 49315, South Korea. (email: cjhwan@dau.ac.kr)

Digital Object Identifier 10.30941/CESTEMS.2021.00018

Therefore, in recent years, an increase in the research on the electrification of the aviation industry has been observed [4-6]. The research theme and roadmap for the aviation electrification ranges from the more electric aircraft (MEA) to the all-electric aircrafts (AEA) [7-8], electric and hybrid propulsion system development for the small and medium range aircrafts.

Considering the broad range for the aviation electrification, the proposed research will limit the discussion for the urban aerial vehicles (UAV) with fixed pitch propellers. The principle component of an UAV is its propulsion system. Similar to the automotive application, the propulsion system of an UAV can either be full electric propulsion (FEP) or hybrid propulsion (HP). Furthermore, the HP can be broadly classified into series and parallel HPs, respectively. In terms of the aircraft types, UAV can have a cantilever low-wing, two-seat side by side configuration or a vertical take-off landing (VTOL) type multicenter with counter rotating propellers. Some recent notable examples of two seat side-by-side models are the Magnus eFusion by Siemens-FlyEco [9], ELIAS by Acentiss [10], ACCEL by Rolls-Royce [11]. Promising candidates for the VTOL multicopter models are CityAirbus by Siemens-Airbus [9], SD-03 by Skydrive [12].

As shown in Fig. 1, the proposed work considers two propulsion architectures of the electric UAV (EUAV), namely, all-electric propulsion and series hybrid propulsion. As shown in Fig. 1(a), in all electric propulsion, an electric motor, usually high-power density permanent magnet synchronous motor (PMSM) is powered by a battery bank. The power conversion stages between the battery and the PMSM contains DC-DC converter, a capacitor bank and an inverter, respectively. For the series hybrid propulsion considering the safety and reliability, a redundant system is considered with a fault tolerant generator-motor set. The generator converts the mechanical power of a diesel engine to electrical power to run the motor. The motor then rotates the aircraft propeller. The power flow between the generator and the motor is achieved using two sets of back to back converters for each redundant winding set. With this idea, the research focus of the proposed work is listed in below:

1) the aim of the proposed work is to devise a fast reliable and integrated design platform for the electric machines used

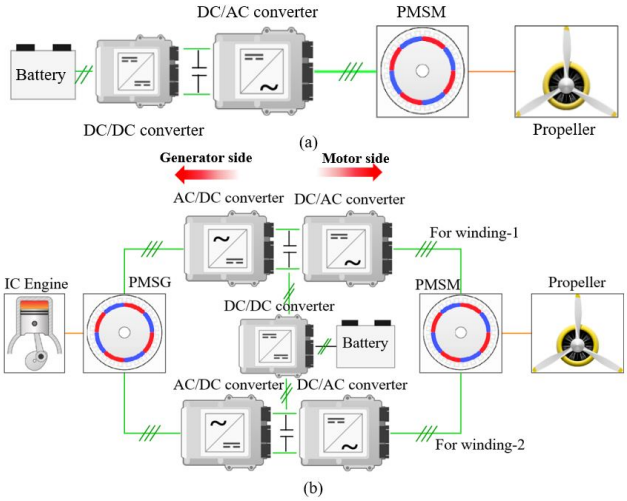

Fig. 1: EUAV propulsion system architecture schematic: (a) All electric propulsion system and (b) redundant series hybrid propulsion system.

for the EUAV propulsion application.

2) The platform should have the power to perform online co-simulation among different blocks of the design steps, namely, electro-magnetic, thermal, mechanical and optimization etc.
3) to serve the purpose, the design platform will feedback data among different commercial design and optimization tools.

As mentioned before, the design process for the high performance electric machines involves different stages. For this proposed work, PMSM will be considered as the targeted machine. Once the initial dimensions are fixed, the design stage of PMSMs starts with the electromagnetic design. traditionally, the electromagnetic design of the PMSM can either be done using (1) the magnetic equivalent circuit (MEC) based linear analytical models or (2) by solving Maxwell's equation using the finite-element method (FEM) with the time stepping scheme. In terms of the accuracy in design result and effect of material nonlinearity, the FEM is superior to the MEC approach. However, in FEM, both temporal and spatial discretization can lead to a large system of equations with an excessively high computational burden. Furthermore, the use of fine meshing techniques and an increased number of time steps result in a decrease in computational efficiency. Therefore, recently to find a computationally efficient alter-native of the conventional FEM based analysis of large scale the electromagnetic systems, approaches based on the *model order reduction* (MOR) have been proposed. Among different available MOR methods, *proper orthogonal decomposition* (POD) based MOR models for different engineering problems are studied extensively [13]-[17]. POD-based MOR uses the *method of snapshots* to generate the optimal basis for the reduced model. As the name suggests, this approach requires to solve the full system for different time steps which are called as the snapshots to create a reduced basis. Similar to the POD-based MOR, another emerging method for the MOR is the use of *Dynamic Mode Decomposition* (DMD). DMD method was initially originated in the fluid dynamic community as a method to decompose complex flow into a simple representation based on spatiotemporal coherent structures [18]-[19]. The central idea of DMD can be thought of

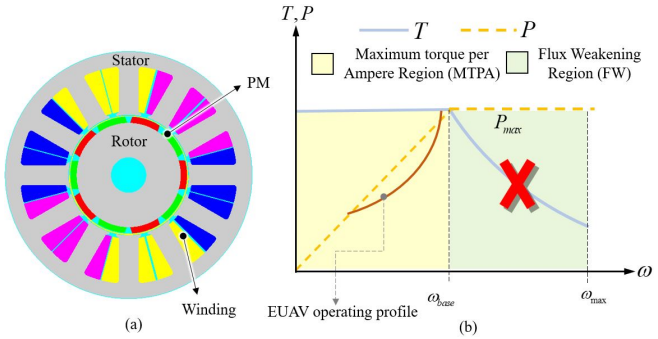

Fig. 2: EUAV PMSM topology: (a) 10P-12S model and (b) Torque-speed characteristics of PMSM and propeller.

as an ideal combination of spatial dimensionality reduction technique such as POD with Fourier transform in time.

In this proposed work, the DMD-based MOR will be used to perform the electromagnetic analysis of the PMSM. The goal is to use the DMD to have a fast-electromagnetic design and couple it to the highly computational genetic algorithm (GA) based optimization platform using MATLAB to have the end-product model of the PMSM. Furthermore, this work aims to show that the DMD model can be effectively used for the noise vibration and harshness (NVH) analysis using *Altair SimLab* and *Optistruct*. A detailed step-by-step discussion will be presented in the following sections.

II. TARGETED PMSM FOR ANALYSIS

The PMSM for the proposed EUAV application is a surface mounted-PMSM (SPMSM) with 10 Poles and 12 Slots as shown in Fig. 2(a). The SPMSM is suitable over interior-PMSM (IPMSM) for the proposed application because for the fixed pitch propeller EUAV applications, the propeller torque is directly proportional to the square of the rotational speed. As a result, the constant torque region of the total torque-speed curve of the PMSM can fulfill the torque demand by the propeller and flux weakening is not needed as shown in Fig 2(b). This is because in the flux weakening region the torque is inversely proportional to the speed and hence does not match with the torque-speed profile of the fixed pitch propeller. Therefore, while driving the propulsor, it should be operated in the constant torque region i.e at maximum torque per ampere (MTPA) drive and by varying the system throttle command using the EUAV controller the required command based on demanded operations such as takeoff, hovering, cruising etc can be generated.

Furthermore, the 10P-12S has a balanced radial force distribution, low torque ripple and cogging torque which is important to ensure the stability of the whole EUAV system. As mentioned before, this work will investigate the effectiveness of DMD to generate a correct simulation model for the proposed PMSM in the following section which is suitable to perform various high-end analysis such as optimization, NVH and thermal analysis on the PMSM.

III. FORMULATION OF DYNAMIC MODE DECOMPOSITION ARCHITECTURE

This paper introduces the use of the dynamic mode decom-

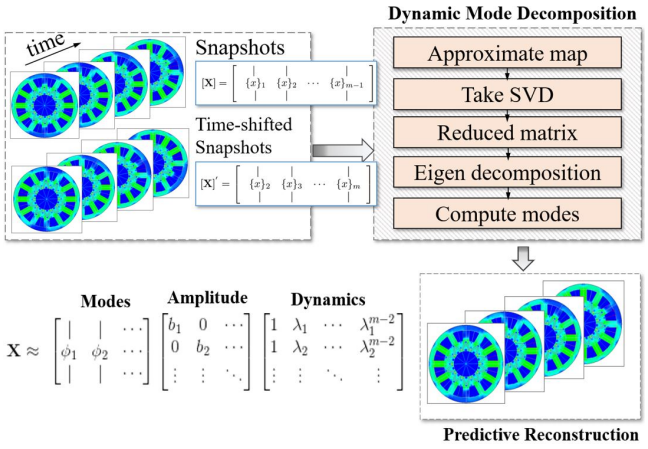

Fig. 3: Schematic of data processing in DMD architecture.

position (DMD) instead of the traditionally used POD based MOR for the dimensionality reduction of electromagnetic modeling of the PMSM. At its core, DMD can be thought of like a combination between the spatial dimensionality reduction techniques such as the POD and Fourier transform in time [7]. The method relies simply on collecting "*snapshot*" of data $\{x\}_k$ from a dynamic system at a number of times t_k where k=1, 2, 3, ...,*m-1*. Furthermore, the data collection process throughout this paper involves two parameters, namely:

1) n = number of spatial points saved per time snapshot.
2) m = number of snapshots taken.

The connection between the state of a linear dynamical system $\{x\}_k$ and to the next step $\{x\}_{k+1}$ can be given as:

$$\{x\}_{k+1} = [\mathbf{P}]\{x\}_k \tag{1}$$

with,

$$[\mathbf{P}] = \exp([P]\Delta t) \tag{2}$$

where, $[P]$ is the continuous-time dynamics matrix. the solution of (1) can be expressed in terms of eigenvalues λ_k and eigenvectors ϕ_k k of the discrete-time map [**P**] as follows:

$$\{x\}_{k+1} = \sum_{j=1}^{r} \phi_j \lambda_j b_j \tag{3}$$

where, $\{b\}$ are the coefficients of the initial condition $\{x\}_1$ in the eigenvector basis. The DMD algorithm finds a low-rank eigendecomposition (3) of the matrix [**P**] that optimally fits the measured trajectory $\{x\}_k$ for k = 1, 2, 3, ..., m in a least square sense so that $\left\|\{x\}_{k+1} - [\mathbf{P}]\{x\}_k\right\|_2$ is minimized across all points for k = 1, 2, 3, ..., m −1.

Now, to find [**P**], suppose two sets of data are avaliable for the dynamical system as follows:

$$[\mathbf{X}] = \begin{bmatrix} | & | & & | \\ \{x\}_1 & \{x\}_2 & \cdots & \{x\}_{m-1} \\ | & | & & | \end{bmatrix} \tag{4}$$

$$[\mathbf{X}]' = \begin{bmatrix} | & | & & | \\ \{x\}_2 & \{x\}_3 & \cdots & \{x\}_m \\ | & | & & | \end{bmatrix} \tag{5}$$

Here, (4) and (5) contains the data sets where the data is stored in such a way that [**X**]' contains the data set one time step ahead of [**X**]. With this, DMD computes a leading eigendecomposition of the best fit linear operator [**P**] relating he data $[\mathbf{X}]' \approx [\mathbf{P}][\mathbf{X}]$ as follows:

$$[\mathbf{P}] = [\mathbf{X}]'[\mathbf{X}] \tag{6}$$

Here, DMD modes are the eigenvectors of [**P**] and each DMD mode corresponds to a particular eigenvalue of [**P**]. A schematic of the data processing architecture using DMD is show in Fig. 3. For practical implementation, algorithm 1 can be used to find the DMD modes. It can further be explained as follows:

Algorithm 1 DMD Algorithm

1: Compute SVD on first data matrix; $[\mathbf{X}] = [\mathbf{U}][\mathbf{\Sigma}][\mathbf{V}]^* \Rightarrow [\mathbf{X}]' = [\mathbf{P}][\mathbf{U}][\mathbf{\Sigma}][\mathbf{V}]^*$
2: Define $[\tilde{\mathbf{P}}] = [\mathbf{U}]^*[\mathbf{A}][\mathbf{U}] = [\mathbf{U}]^*[\mathbf{X}]'[\mathbf{V}][\mathbf{\Sigma}]^{-1}$
3: compute eigendecomposition of $[\tilde{\mathbf{P}}]$, $[\tilde{\mathbf{P}}][\mathbf{W}] = [\mathbf{W}][\mathbf{\Lambda}]$. (where, $[\mathbf{W}]$ is the matrix of eigenvectors, and $[\mathbf{\Lambda}]$ is the diagonal matrix of eigenvalues. Each eigenvalue λ_i is a DMD eigenvalue.)
4: Compute the DMD modes, $[\mathbf{\Phi}] = [\mathbf{X}]'[\mathbf{V}][\mathbf{\Sigma}]^{-1}[\mathbf{W}]$ (Each column of $[\mathbf{\Phi}]$ is a DMD mode ϕ_i corresponding to eigenvalue λ_i.)

1) First, perform the SVD of [**X**].

$$[\mathbf{X}] = [\mathbf{U}][\Sigma][\mathbf{V}]^* \tag{7}$$

where, $\mathbf{U}_{n\times r}$ and $\mathbf{V}_{m\times r}$ are two orthogonal matrices and $\Sigma_{r\times r}$ is a diagonal matrix containing non-negative singular values. Here, r is the rank of the reduced SVD approximation to [**X**] and [**U**] gives the POD modes. The SVD is included in the first step of the algorithm because it provides the low-rank truncation of the data. Specifically, if the low-rank truncation is available, [Σ] will decrease sharply to zero with a limited number of dominant nodes.

2) Matrix [**P**] from (6) can be obtained by using the pseudoinverse of [**X**] obtained in first step:

$$[\mathbf{P}] = [\mathbf{X}]'[\mathbf{V}][\Sigma]^{-1}[\mathbf{U}]^* \tag{8}$$

However, for the practice purpose, it is more computationally efficient to compute a r×r projection $[\widetilde{\mathbf{P}}]$ of full matrix [**P**] onto POD modes:

$$[\widetilde{\mathbf{P}}] = [\mathbf{U}]^*[\mathbf{P}][\mathbf{U}] = [\mathbf{U}]^*[\mathbf{X}]'[\mathbf{V}][\Sigma]^{-1} \tag{9}$$

Here, $[\widetilde{\mathbf{P}}]$ defines a low-dimensional linear model of the the dynamic system on POD coordinates:

$$\{\tilde{x}\}_{k+1} = [\widetilde{\mathbf{P}}]\{\tilde{x}\}_k \tag{10}$$

Compute the eigendecomposition of $[\widetilde{\mathbf{P}}]$ as shown in algorithm 1.

Finally from the eigendecomposition, using the eigen-vector [**W**] and the eigenvalues [Λ], reconstruction of the eigendecomposition of [**P**] can be done. In particular, [Λ] gives the eigenvalues of [**P**] and the DMD modes are given by the columns of [Φ], where [Φ] can be written as:

$$[\Phi] = [\mathbf{X}]'[\mathbf{V}][\Sigma]^{-1}[\mathbf{W}] \tag{11}$$

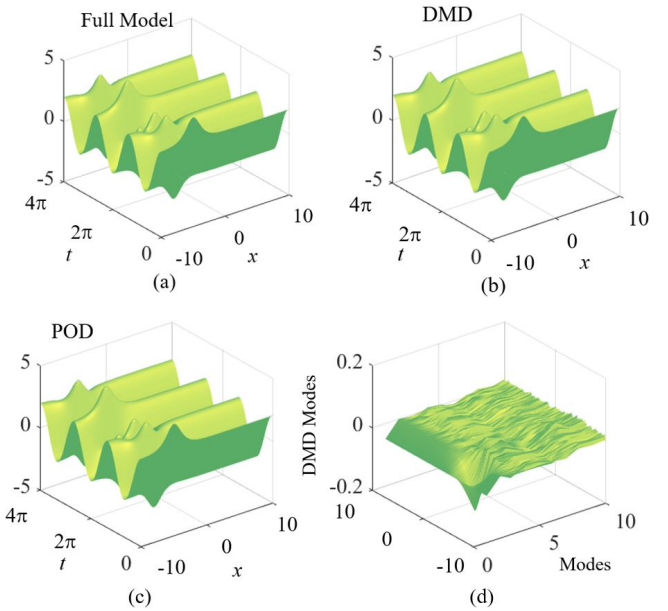

Fig. 4: Example of spatio-temporal dynamics of a function and the capability of MOR to reproduce the full model: (a) Full model, (b) DMD, (c) POD and (d) DMD modes for reconstruction.

Now with this low-rank approximations of the both the eigenvalues and the eigenvectors available using the algorithm 1, the projected future solution of the specific problem can be constructed for all times in the future solution. Thus the approximate solution at all the future times can be given as follows:

$$\{x\}(t) \approx \sum_{k=1}^{r} \phi_k \exp(\omega_k t) b_k = \Phi \exp(\Omega t)\mathbf{b} \qquad (12)$$

where, b_k is the initial amplitude of each mode, [Φ] is the matrix whose columns are the DMD modes and [Ω] is a diagonal matrix whose entries are the eigenvalues ω_k. With this idea, in the following sections, DMD method is utilized to study a quasi-magetostatic problem.

IV. APPLICATION

A. Numerical Example

$$f(x,t) = \operatorname{sech}(x+5)\exp(j3.7t) + \operatorname{sech}(x) + \cosh(x)\exp(j1.5t) \qquad (13)$$

for (13), $x \in [-10,10]$ and $t \in [0,4\pi]$ respectively. Fig. 2(a) shows the high rank full model spatiotemporal distribution of the function in (13). The approximated model reconstruction in Fig 2(b) and 2(c) shows the rank-2 truncation MOR models generated using the proposed DMD and traditional POD method. Furthermore, rank 2 truncation is selected because it can be seen from the singular value energy distribution in Fig. 3(a), around 99% of the total energy is stored in the first two modes. Therefore, these two modes would be enough to reconstruct the MOR models. Moreover, the DMD modes up to 10 ranks, used for the linear reconstruction is shown in Fig. 2(d). It is mentioned above that DMD has the capability to preserve both the spatial and the temporal characteristic of the full model. Thus, in Fig. 3 (b) and (c), the temporal modes for first two ranks of the DMD and the POD are compared with the full model. And it can be seen that DMD is much superior in preserving the temporal characteristics which will result in a lower mode error calculated with l_2 norm. Thus, it can be said that DMD is efficient in decomposing spatiotemporal data. With this, in the following section DMD is implemented First on a quasi-magetostatic problem, i.e *Team problem* $21^a - 0$ [8], then implemented on the proposed PMSM modeling.

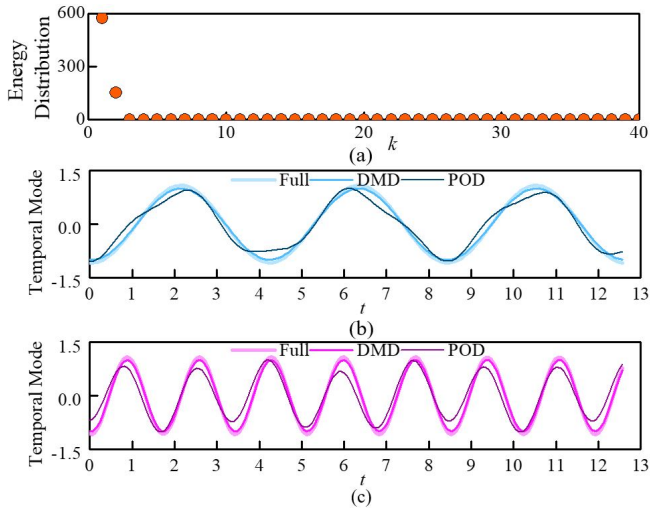

Fig. 5: (a) singular values showing a rank-2 trancation is appropriate,(b) Mode-1 temporal modes for full, DMD and POD model, (c) Mode-2 temporal modes for full, DMD and POD model.

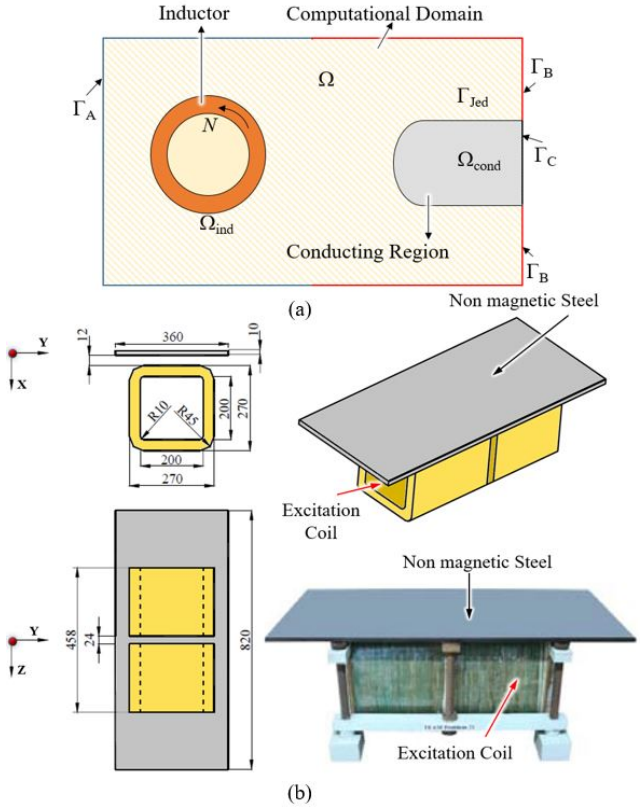

Fig. 6: Spatial domain of quasi-magnetostatic problem.

TABLE I
SPECIFICATION OF MODEL

Parameters	Values
Number of turns of each coil	300
Conductivity of wire	5.7143×10^7 kg/m^3
Density of wire	8.9×10^3 kg/m^3
Rated excitation current	±10A (50Hz, rms)

B. Quasi-magnetostatic Problem

To have the basic idea of a quasi magnetostatic problem, as shown in Fig. 6 a domain Ω is considered. The boundary of Ω can be defined as $\Gamma = \Gamma_A \cup \Gamma_B$ and $\Gamma_A \cap \Gamma_B = 0$. The domain Ω includes a stranded inductor Ωind and a conducting subdomain Ω_{cond} with a boundary of $\Gamma_{cond} = \Gamma_C \cup \Gamma_{Jed}$ the solving scenerio for this problem statement can be given as $x \in \Omega$ and $t \in [0,T]$.

To solve a quasi-magnetostatic problem, the method of vector potential can be used. Vector potential $\{A\}$ for the domain Ω can be defined using Maxwell's equation as follows:

$$\text{curl}\frac{1}{\mu}\text{curl}\{A\}(x,t)+\sigma\frac{\partial\{A\}}{\partial t}=\{N\}(x)i(t) \quad (14)$$

where, μ is the magnetic permeability, σ is the electrical conductivity, $\{N\}$ is the unit current density vector and $\{i\}$ is the current flowing through the stranded inductor. Applying Galerkin method to (14), a system of ordinary differential equation can be obtained as follows:

$$[\mathrm{M}]\frac{\mathrm{d}\{X\}(t)}{\mathrm{d}t}+[\mathrm{K}]\{X\}(t)=\{\mathrm{F}\}i(t) \quad (15)$$

where, unknown vector $\{X\}(t)$ contains the values of $\{A\}$ along all edges of the mesh. To (15), when MOR is applied, the reduced order system of equation can be rewritten as:

$$[\mathrm{M}_r]\frac{\mathrm{d}\{X_r\}(t)}{\mathrm{d}t}+[\mathrm{K}_r]\{X_r\}(t)=\{\mathrm{F}_r\}i(t) \quad (16)$$

where, $[\mathrm{M}_r]$, $[\mathrm{K}_r]$ and $\{\mathrm{F}_r\}$ are the reduced order approximation of the full model components in (15). To find these reduced order approximations, proposed DMD method is implemented based on the algorithm 1. To verify *TEAM Problem* $21^a - 0$ is used an example.

C. Validation with TEAM Problem $21^a - 0$

To validate the effectiveness of DMD in approximating quasi-magnetostatic models, *TEAM Problem* $21^a - 0$ is used as a reference system [20]. As shown in Fig. 6(a)-(b), the computational model is a linear eddy current model with multiple connected regions. There are two coils of same specifications with excitation currents flowing in the opposite directions and a nonmagnetic steel plate. The geometrical specifications are shown in Fig. 6(b) with other essential specifications of the systems listed in Table I. The boundary condition of the model is the Dirichlet condition and a zero initial condition is considered. The domain is divided by quadrilateral elements, where number of nodes are 9605. The discrete time step, Δt is taken as 0.0002s. To analyze, first 200 solutions solved by (15) are selected as snapshots. Using these, based on the DMD algorithm mentioned in section II, DMD reduced order basis is calculated. Fig. 7 shows the energy distribution or singular value distribution showing dominant modes which can be used to reconstruct the reduced model of the system. As shown in energy distribution plot of Fig. 7, the reconstruction using DMD is possible only by using the first mode, which is the dominant mode here. Thus, with DMD mode, $r = 1$, approximation of the system is done. Fig. 8 shows the first 25 snapshots of the magnetic vector potential for the full and DMD-MOR model (r=1). It is interesting to note that

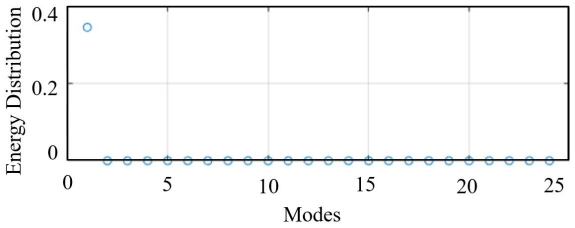

Fig. 7: Singular value spectrum for first 25 modes showing rank-1 truncation approximation in normal and logarithmic scale.

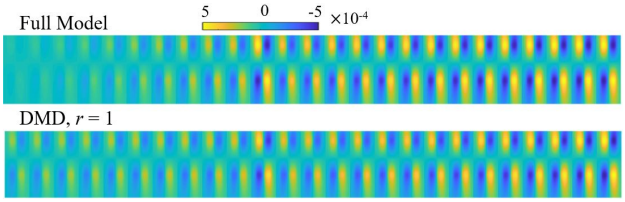

Fig. 8: First 25 snapshots of the vector potential for the full and the DMD(r = 1) models.

DMD based MOR has very efficiently reconstructed the full model with a l_2 norm error of 1.38 × 10−07. Furthermore, when compared with the traditional POD method, the mode error between the POD and the full model was in 40% whereas the mode error is negligible in case of DMD

DMD(r = 1) models.

D. Implementation on Proposed PMSM Modeling

In this section, DMD is implemented on the proposed 10P-12S PMSM for the EUAV as shown in Fig. 2(a). The computational domain of the PMSM can be designed as shown in Fig. 9. For comparison with the full model obtained using Finite Element Analysis (FEA), the air gap flux density at the stator tooth inner surface is considered. This information will be used in later stage to calculate radial force using *Maxwell's Stress Tensor* analysis. At base speed of 1000 RPM with rated current value of 70.7 A_{rms}. The analysis is performed at the *maximum torque per ampere* (MTPA) point of the PMSM. The other machine parameters are mentioned in Table II. The magnetic flux density distribution is shown in Fig 10(a). The flux density is measured at the A-phase current peak point. Fig. 10(b) shows the spatial distribution of the *radial* and *tangential* flux densities. A comparison of the average value of the flux density components obtained using DMD and full model using FEA are presented in Table III. As shown in Table III, the deviation between the DMD and FEA results are below 2%. This proves again the ability of the DMD to correctly provide the electromagnetic model of the PMSM. Furthermore, only rank 4 approximation is used to generate the DMD model. Thus, it provides an advantage of obtaining very fast analysis result compared to the traditional FEA based models.

To understand the proper applicability of the proposed DMD model of the PMSM for EUAV, in the following sections examples highlighting the co-simulation of the proposed DMD model of the PMSM with high end analysis such as the optimization tool and NVH analysis will be performed.

V. USE OF DMD-BASED PMSM MODEL IN HIGH-END DESIGN ANALYSIS

Once the electromagnetic design is performed, the PMSM

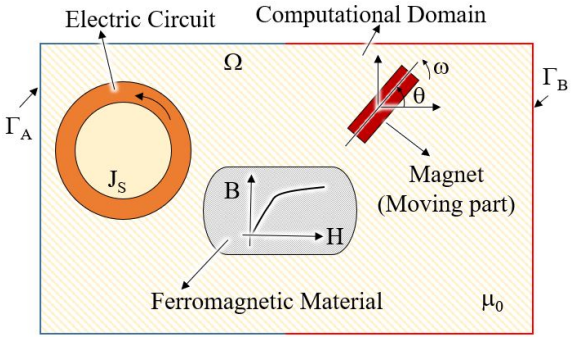

Fig. 9: Computational domain schematic for the proposed PMSM.

TABLE II
PROPOSED PMSM ANALYSIS CONDITIONS

Parameters	Values
Current(Arms)	70.7
Current angle	0
Magnet remanent flux densitt	1.2
Core material	35PN230(POSCO)
Turn per phase	320
Strand in Hand	2

TABLE III
AVERAGE VALUES FLUX DENSITY COMPONENTS

Parameters	FEAs	DMD	Deviation(%)
Radial flux density	1.1	1.08	1.8
Tangential flux density	0.7	0.69	1.4

should undergo a set of high-end design analysis such as the *optimization process, noise, vibration and harshness* (NVH) analysis and *thermal characteristic design* before sending for production. This section will discuss the applicability of the DMD-model of the proposed PMSM in studying the optimization and NVH characteristic and try to establish a closed loop analysis platform for studying the whole process online.

A. Co-simulation with Optimization Process

This section aims to create a co-simulation model between the DMD-based PMSM model and the *genetic algorithm* (GA)-based parametric optimization under a single platform using MATLAB-Simulink. The flow-chart for the DMD and GA combined platform is shown in Fig. 11. As shown in Fig. 11, the DMD model is used as a base model to create the optimized final model using a *response surface moment based reliability-based design optimization* (RBDO).it is to note that, this optimization platform is not a traditional geometric optimization, rather it considers the manufacturing tolerances in the design process. The GA in the proposed architecture considers a uniform distribution of the design parameters. This co-simulation platform can consider different design optimization scenarios such as the (1) deterministic optimization (using only the DMD- model) which does not account for the manufacturing uncertainties of the design parameter and (2) RBDO, whereby the tolerance effects of the design parameters (from machines with ± 0.05 mm and ± 0.1 mm tolerances) are considered during the optimization with near negligible failure probability of P_t = 0.01 % [21]. Furthermore, the design platform uses *Monte Carlo* (MC) simulation to calculate the actual constraint non-compliance.

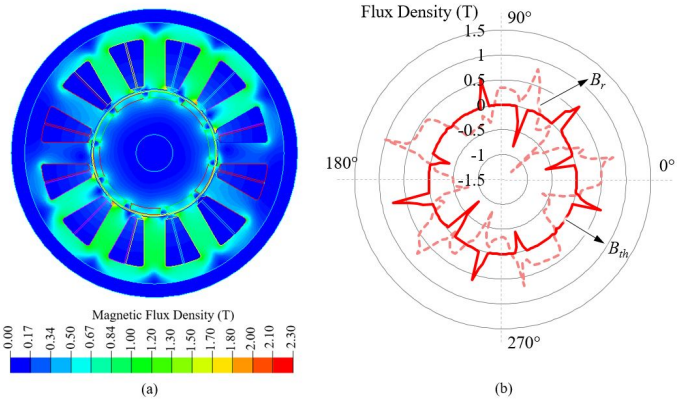

Fig. 10: (a) Flux-density distribution of the proposed PMSM obtained using DMD and (b) radial and tangential flux density distribution.

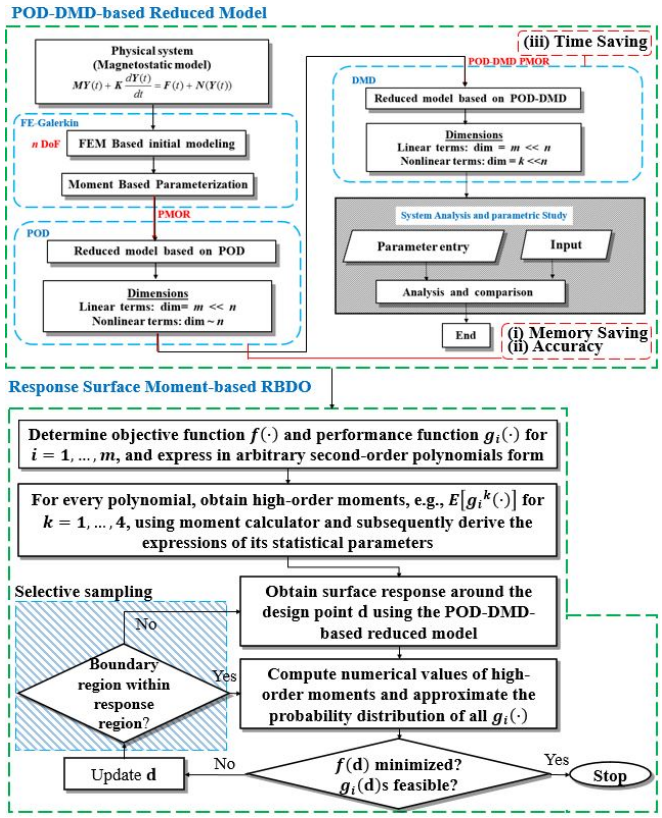

Fig. 11: Co-simulation between the DMD-based electromagnetic model and the genetic algorithm based optimization considering the manufacturing uncertainty.

It is well-known that GA takes a longer time to provide the optimized model as it is a computationally heavy process and if combined with the FEA, it is challenging in terms of the simulation time, computational efficiency and the technical requirement of the computational system. However, the process shown in Fig. 11 takes the rank reduced DMD model to eliminate the computation burden and makes the whole design process faster. A model call reduction of approximately 15% can be achieved by using DMD compared to the FEA. This proves the need and usability of DMD based modeling for the high-end design of the high-performance PMSMs for EUAV applications.

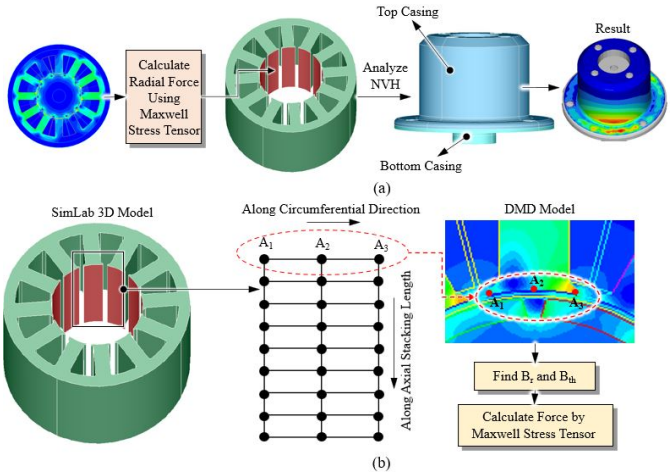

Fig. 12: NVH calculation of the proposed PMSM by mapping the electromagnetic force from the maxwell stress tensor analysis of the proposed DMD model to the SIMLAB structural software model of the stator.

B. *Co-simulation with NVH Tool*

In PMSM machines the magnetic force that exists on the interface between the air gap and the ferromagnetic sections such as the stator or rotor can create severe motor vibration with annoying noise. In terms of the EUAV safety and reliability, a PMSM with high redial force is not desired. Thus it is important to perform the NVH analysis on the PMSM and its casing to check and understand the source of noise and vibration and reduce it. This section discusses the use of DMD model of the PMSM to perform a cosimulation on NVH using DMD coupled with *Optistruct* tool by Altair. To co-simulation steps are shown in Fig. 12 (a). As shown in Fig. 12(a), the DMD model is used to calculate the radial, tangential and resultant magnetic force on the stator tooth surface which can then be mapped to the 3D structural model of the Stator in the Simlab structural software by Altair. It is important to consider that the mapping between the DMD model and the Simlab 3D model should be same with correct node to node linking. For an example, as shown in Fig. 12(b), if a grid with three nodes along tooth circumferential direction and nine nodes along axial stacking direction is considered, the the radial and tangential flux densities *i.e* B_r and B_{th} information on these nodes should be obtained. As shown in Fig. 12(b), the spatial flux density information of the DMD model on these nodes can be used to create an matrix containing the B_r and B_{th} values which can then be used to find the resultant flux density vector and the radial force by using the *Maxwell's Stress Tensor* method. This force information can then be feedback to the Simlab model to calculate the effect of radial force in creating the NVH. Spatial distribution of the radial, tangential and resultant force vectors are shown in Fig. 13. In the NVH analysis, it is considered that the PMSM casing is connected to fixed surface on bottom casing side and to the propeller on the top casing side, which serves as the boundary condition for the analysis. Fig. 14 (a) shows different eigen modes obtained using the NVH analysis. *Equivalent radiated power* (ERP) is shown in Fig. 14(b). ERP is an IEEE standardized definition of directional radio frequency (RF) power which provides the exterior sound radiation distribution by the PMSM housing. This analysis

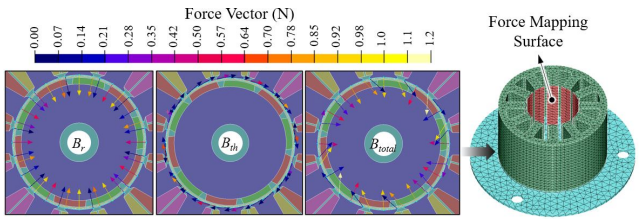

Fig. 13: Radial, tengential and resultant force vectors on the stator tooth surface of the proposed PMSM.

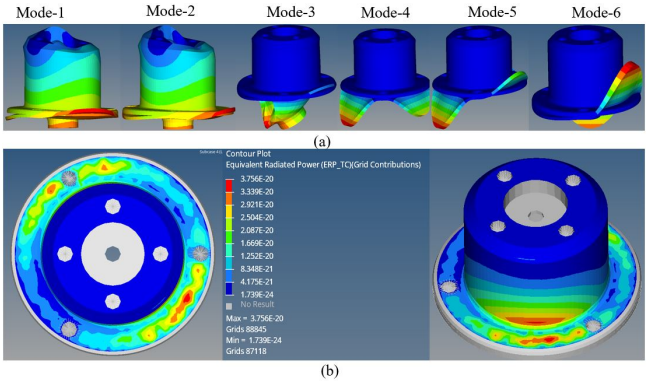

Fig. 14: NVH analysis : (a) Eigen modes analysis on the stator outer casing and (b) Equivalent rediated power distribution.

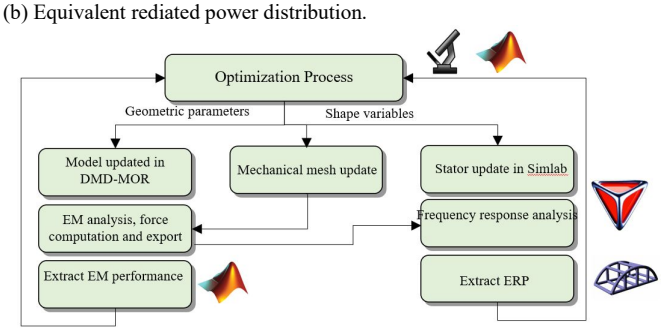

Fig. 15: Multi-physics Motor Optimization for Noise Reduction.

again proves the applicability of DMD in performing structural analysis such as NVH in a feedback environment with other commercial tools.

Finally, Fig. 15 shows a closed-loop environment architecture combining DMD with Matlab, Altair hyperstudy, Simlab and optistruct which can be developed combining the discus-sions in section V-B and V-C. This platform provides the users a fast model based design approach to optimize the PMSM for noise reduction and structural stability. This design process is under construction, therefore is not detailed in this work.

VI. CONCLUSION

In this paper, the architecture and performance of the Dynamic Mode Decomposition (DMD)-based MOR for the design and analysis of the permanent magnet synchronous motor (PMSM) for Electric Urban Aerial Vehicle (EUAV) Propulsion is proposed. The targeted design approach of the proposed work can be summarized as follows:

1) A detailed DMD algorithm making scheme is presented in the work which is first tested on a numerical spatiotemporal function and then applied directly on the TEAM Problem 21^a – 0 to check its effectiveness to solve the quasi-magnetostatic

problem efficiently and then implemented in developing electromagnetic model of the PMSM for EUAV.

2) The targeted aim was to find a more computationally efficient substitute of the tradition Finite element analysis (FEA). It is found that DMD results in lower mode error compared to the other traditional methods when l_2 norm difference is calculated with respect to the full model.

3) Furthermore, other design methodologies with high-end analysis for end-product design such as the optimization, noise-vibration and harshness (NVH) analysis at co-simulation with the DMD model are also studied to provide the readers an idea on the usefulness of DMD.

The future goal is to incorporate DMD to thermal analysis to create successful closed-loop platform to perform electromagnetic-structural-thermal modeling as a model-based design of the PMSM for EUAV.

REFERENCES

[1] Blaabjerg F, et al. “High Power Electronics: Key Technology for Wind Turbines. In: Power electronics for renewable energy systems, transpori-tation and industrial application”, Wiley-IEEE Press, 1st ed., 2014.

[2] J. Ribeiro et al. “Environmental assessment of hybrid-electric propulsion in conceptual aircraft design”, *Journal of Cleaner Production*, vol. 247, Art. No. 119477, 2020.

[3] “Flightpath 2050 Europe’s Vision for Aviation-Report of the High Level Group on Aviation Research”, European Commission, 2011.

[4] D. Sziroczak et al. “Conceptual design of small aircraft with hybrid-electric propulsion systems”, *Energy*, vol. 204, Art. No. 117937, 2020.

[5] O. Zaporozhets et. al. “Trends on current and forecasted aircraft hybrid electric architectures and their impact on environment”, *Energy*, vol. 211, Art. No. 118814, 2020.

[6] V. Madonna et al. “Electrical Power Generation in Aircraft: Review, Chal-lenges, and Opportunities”, *IEEE Trans. Transportation Electrification*, vol. 4, No. 3, 2018.

[7] B. Sarlioglu et al.”More Electric Aircraft: Review, Challenges, and Oppor-tunities for Commercial Transport Aircraft”, *IEEE Trans. Transportation Electrification*, vol. 1, No. 1, 2015.

[8] J. K. Noland et al. “High-Power Machines and Starter-Generator Topolo-gies for More Electric Aircraft: A Technology Outlook” *IEEE Access*, vol. 8, 2020.

[9] eAircraft: hybrid electric propulsion systems for aircraft-Siemens AG 2019.

[10] The future of electrically-powered flight-Elias, Acentiss https://www.acentiss.de/luftfahrt/luftfahrt-elektrisches-fliegen

[11] ACCEL: entering the era of zero-emissions aviation, Rolls Royce, https://www.rolls-royce.com/innovation/key-demonstrators/accel.aspx

[12] SD-03 -SkyDrive, http://en.skydrive2020.com/air-mobility/

[13] A. Pierquin, T. Henneron, S. Clenet, S. Brisset, ”Model-order reduc-tionof magnetoquasi-static problems based on POD and Arnoldi-based Krylov methods,” *IEEE Trans. Magn.*, vol. 51, no. 3, Mar. 2015, Art. no. 7206204.

[14] D. S. Schmidth¨ausler, S. Sch¨ops, M. Clemens, ”Linear subspace reduc-tion for quasistatic field simulations to accelerate repeated computations”, *IEEE Trans. Magn*., vol. 50, no. 2, Feb. 2014.

[15] Y. Sato, F. Campelo, and H. Igarashi, “Fast shape optimization of antennas using model order reduction,” *IEEE Trans. Magn*., vol. 51, no. 3, Mar. 2015, Art. no. 7204304.

[16] Laurent Montier, Thomas Henneron, Benjamin Goursaud, St´ephane Cl´enet, ”Balanced Proper Orthogonal Decomposition Applied to Magnetoquasi-Static Problems Through a Stabilization Methodology”, *IEEE Trans. Magn*., vol. 53, no. 7, pp. 1-10, 2017.

[17] Kenta Kuriyama, Akihisa Kameari, Hassan Ebrahimi, Takayuki Fu-jiwara, Kengo Sugahara, Yuji Shindo, Tetsuji Matsuo, ”Cauer Ladder Network With Multiple Expansion Points for Efficient Model Order Reduction of Eddy-Current Field”, *IEEE Trans. Magn.*, vol. 55, no. 6, pp. 1-4, 2019.

[18] B. W. Brunton,, et al. ”Extracting spatial-temporal coherent patterns in large-scale neural recordings using dynamic mode decomposition.” *Journal of neuroscience methods*, vol. 258, pp. 1-15, 2016.

[19] J. H. Tu, C. W. Rowley, D. M. Luchtenburg, S. L. Brunton, and J. N. Kutz, “On dynamic mode decomposition: Theory and applications,” *J. Comput. Dyn*., vol. 1, no. 2, pp. 391–421, 2014.

[20] Z. Cheng et al. ”TEAM problem 21 family (V. 2009)”, available at: www.compumag.org/jsite/team, approved by the International Compumag Society at Compumag 2009.

[21] S Paul et al. “Parametric Design Analysis of Magnetic Sensor Based on Model Order Reduction and Reliability-Based Design Optimization”, *IEEE Trans Magn*. vol. 54, no. 3, 2018.

Sarbajit Paul received the M.Sc. degree in electrical engineering in 2016 from the Mechatronics System Research Laboratory, Department of Electrical En-gineering, Dong-A University, Busan, South Korea, where he is currently working toward the Ph.D. degree in high-power permanent magnet machine design. His current research interests include perma-nent magnet generator design, drives, and actuators.

Mr. Paul was a Korean Government Research Scholar, under Ministry of Education, South Korea, from 2014 to 2016. He received the Australia Award Endeavour Research Fellowship from 2017 to 2018 to perform part of his research at the University of New South Wales. He is a Student Member of different IEEE societies such as IEEE Industrial Electronics Society (IES), IEEE Industry Applications Society (IAS), and IEEE Robotics and Automation Society (IRA), and a member of IES Technical Committee on control, robotics and mechatronics. He was a recipient of the 2016 Travel Grant Award by the IEEE Instrumentation and Measurement Society and the 2017 Best Research Paper Award by the IEEE Region 10 (Asia-Pacific), 2017, 2020 Best Research Paper Award by KIEE.

Junghwan Chang received the B.S. and M.S. de-grees in electrical engineering and the Ph.D. degree in precision mechanical engineering from Hanyang University, Seoul, South Korea, in 1994, 1997, and 2001, respectively.

From 2001 to 2002, he was with the Institute of Brain Korea 21, Hanyang University, where he developed micro drive and high-speed spindle motor. From 2002 to 2003, he was a Research Fellow with the University of California at Berkeley, Berkeley, CA, USA, where he analyzed and developed electrically controlled engine valve system. From 2003 to 2009, he was a Technical Leader with the Korea Electrotechnology Research Institute, South Korea, where he was involved in the developments of

special purpose machines. Since 2009, he has been a Professor with the Department of Electrical Engineering, Dong-A University, Busan, South Korea. His current research interests include the design and analysis of electromechanical systems, such as electrically driven machine tools, and magnetic gear.

Dr. Chang is a member of The Korea Institute of Electrical Engineers, South Korea. He was a Steering Committee Member and the Technical Program Chair in different conferences, such as International Conference on Electrical Machines and Systems (ICEMS) 2013, IEEE International Transportation Electrification Conference Asia-Pacific 2016, COMPUMAG 2017, and ICEMS 2018. He is a Reviewer of the IEEE TRANSACTIONS ON MAGNETICS, IEEE TRANSACTIONS ON INDUSTRIAL ELECTRONICS, IEEE TRANSACTIONS ON INDUSTRIAL APPLICATION, IEEE/ASME TRANSACTIONS ON MECHATRONICS etc.